Buried particulate organic C fuels heterotrophic metabolism in the hyporheic zone of a montane headwater stream

Satish P. Serchan[1,2,5], Steven M. Wondzell[1,6], Roy Haggerty[2,7], Robert Pennington[2,8], Kevin Feris[3,9], Angelo Sanfilippo[3,10], Daniele Tonina[4,11], and W. Jeffery Reeder[4,12]

[1]United States Department of Agriculture Forest Service, Pacific Northwest Research Station, 3200 Southwest Jefferson Way, Corvallis, Oregon 97331 USA
[2]College of Earth, Ocean, and Atmospheric Sciences, Oregon State University, Corvallis, Oregon 97331 USA
[3]Department of Biological Sciences, Boise State University, Boise, Idaho 83725 USA
[4]Center for Ecohydraulics Research, University of Idaho, Boise, Idaho 83702 USA

Abstract: We examined the interactions between stream water and subsurface sediment to quantify how these interactions influenced organic C respiration and dissolved inorganic C (DIC) production in the hyporheic zone of a high-gradient headwater mountain stream draining a forested catchment at the H. J. Andrews Experimental Forest, Oregon, USA. We compared measurements from a well network with those from six 2-m-long hyporheic mesocosms. The patterns in hyporheic metabolism were similar in wells and mesocosms: O_2 declined and DIC increased with travel time. However, the dissolved organic C (DOC) showed little net change in concentration. The mesocosms showed that net losses of DOC could account for 7% of O_2 consumed during summer and autumn and 24% of O_2 consumed in the winter and spring. Previous research at our study site suggested that large volumes of hyporheic exchange are likely to result in continual processing of streamwater DOC through the hyporheic zone, which would limit the accumulation of bioavailable DOC. Consequently, hyporheic respiration in this forested headwater stream appears to rely primarily on organic C ultimately derived from sediment-bound or buried particulate organic matter (POC). We modeled the consumption of O_2 (k_{O2}) and the production of DIC (k_{DIC}) as zero-order kinetic reactions. In the mesocosms, k_{O2} and k_{DIC} were correlated to temperature and were 2× higher in the summer and autumn than in the winter and spring. In the well network, however, neither k_{O2} nor k_{DIC} showed seasonal differences. The k_{DIC} was also correlated to initial DOC concentrations in both the mesocosms and the wells. Further, the k_{DIC} was correlated to the time since the mesocosms were packed, which suggests that sediment disturbance or incorporation of relatively fresh organic matter from packing the mesocosms increased the bioavailability of the POC. Further, changes in concentrations of O_2, DOC, and DIC were approximately linear when plotted against travel time for both the mesocosms and the well field. These data suggest that the processes that release bioavailable DOC from POC are relatively constant along hyporheic flow paths and govern the rate of hyporheic metabolism in the hyporheic zone of this forested headwater stream.

Key words: hyporheic, mesocosm, aerobic respiration, dissolved organic carbon, DOC, particulate organic carbon, POC, headwater stream

The hyporheic zone is the zone of saturated sediment beneath and adjacent to streams where stream water flows from the surface channel into the subsurface and reemerges at a downstream location. The hyporheic zone can be a critical site for organic C processing (Findlay et al. 1993, Battin 1999, Corson-Rikert et al. 2016). The mixing of stream water with deep groundwater or soil water draining from adjacent hillslopes and the long contact times with metabolically active biofilms on sediment allow oxidation of organic C (Stegen et al. 2016). Both dissolved organic C (DOC) and particulate organic C (POC) are metabolized in the hyporheic zone (Grimm and Fisher 1984, Findlay et al. 1993,

E-mail addresses: [5]satish.serchan@gmail.com; [6]To whom correspondence should be addressed, steven.wondzell@usda.gov; [7]rhaggerty@lsu.edu; [8]robertopennington@gmail.com; [9]kevinferis@boisestate.edu; [10]angeloryansanfilippo@gmail.com; [11]dtonina@uidaho.edu; [12]reed4827@vandals.uidaho.edu

Received 8 September 2023; Accepted 20 February 2024; Published online 2 August 2024. Associate Editor, Robert Payn.

Freshwater Science, volume 43, number 3, September 2024. https://doi.org/10.1086/731772

Pusch 1996, Baker et al. 1999, Brugger et al. 2001, Sobczak and Findlay 2002). Consequently, the hyporheic zone can be a sink for organic C within the stream environment (Battin et al. 2003), and the metabolism of organic C can be a source of dissolved inorganic C (DIC) to the stream (Argerich et al. 2016).

C dynamics within the hyporheic zone vary with space and time because of the extent of mixing of different source waters (Schindler and Krabbenhoft 1998, Battin 1999, Baker et al. 2000) and biogeochemical processes that occur in the flood plain and the hyporheic zone (Findlay et al. 1993, Jones et al. 1995a, Shibata et al. 2001, Corson-Rikert et al. 2016). Mixing of different water sources is generally controlled by interactions between geomorphic and hydrologic settings of streams (Cardenas and Wilson 2006, Poole et al. 2006, Ward et al. 2012, Wondzell and Gooseff 2013, Hester et al. 2017). Further, hyporheic flow paths extend over a wide range of spatial and temporal scales (Harvey and Bencala 1993, Wondzell and Swanson 1999, Kasahara and Wondzell 2003, Malzone et al. 2016, Ward et al. 2016) which in turn influences biogeochemical processes. Short timescale hyporheic exchange flows can provide a continuous supply of dissolved O_2 and DOC to the hyporheic zone, which can stimulate heterotrophic metabolic activity (Findlay et al. 1993). DIC accumulates along hyporheic flow paths from metabolic activity and, perhaps, from mixing with groundwater rich in DIC. The distal ends of long hyporheic flow paths may become anoxic and dominated by anaerobic pathways of C metabolism (Hedin et al. 1998, Baker et al. 1999). Some studies have shown that DOC can accumulate along anaerobic flowpaths, including both CH_4 and other compounds produced from buried organic matter (Schindler and Krabbenhoft 1998, Helton et al. 2015). The C fluxes from riparian and hillslope flow paths to streams are likely to vary seasonally (e.g., during snow melt in alpine streams; Battin 1999), and C flushed from the shallow subsurface can stimulate hyporheic metabolism (Baker et al. 2000). Similarly, soil CO_2 produced from root respiration and oxidation of organic matter in the vadose zone can contribute DIC (Tsypin and Macpherson et al. 2012). The flux of DIC from the vadose zone could be enhanced by diffusion into water films on sediment at the boundary of the capillary fringe. Subsequently, this water could be advected into the hyporheic zone as the height of the water table fluctuates in response to diurnal cycles of evapotranspiration (Corson-Rikert et al. 2016).

Our study focuses on the hyporheic zone of Watershed 1 (WS01), a small stream in a mountainous headwater catchment located in the H. J. Andrews Experimental Forest in western Oregon, USA. Simulations of hyporheic exchange using groundwater flow models showed that step-pool sequences were primary drivers of hyporheic exchange flows, that all of the water in the stream would cycle through the hyporheic zone in as little as 50 m of channel length during late-summer low flow (Wondzell 2011), and that the distribution of residence times of stream water in the hyporheic zone was skewed towards short residence times with a median residence time of 18 h (Kasahara and Wondzell 2003). Analysis and results from other tracer studies found strong persistence of near-stream hyporheic exchange across a wide range of base flow conditions (Wondzell 2006, Ward et al. 2016). Further, flow direction through the valley floor was strongly down valley and varied little across a wide range of observed discharges, from low baseflow to storm flows (Voltz et al. 2013). However, intrusion of soil water from the adjacent hillslopes into the valley floor increases under wetter conditions (Schmadel et al. 2017, Pennington 2019), contracting the spatial extent of the hyporheic zone. Previous investigation of C dynamics in WS01 demonstrated that the hyporheic zone is metabolically active (Corson-Rikert et al. 2016), and as much as $^1/_3$ of the stream's annual DIC flux may be sourced from the hyporheic zone in this catchment (Argerich et al. 2016).

The objective of our study was to examine the interactions between stream water and subsurface sediment in WS01 to better quantify how these interactions influenced organic C respiration and DIC production in the hyporheic zone. These processes are difficult to isolate in situ because the hyporheic zone is influenced by mixing of different source waters as well as interactions with the overlying soils and riparian vegetation. Therefore, we designed hyporheic mesocosms to isolate simulated near-stream hyporheic flow paths. Using the mesocosm, we asked: Is stream-sourced DOC or sediment-bound or buried POC more important in fueling heterotrophic metabolism in this hyporheic zone?

METHODS

We designed hyporheic mesocosms to simulate near-stream hyporheic flow paths and used them to examine the respiration of stream-sourced DOC and sediment-bound or buried POC. From 2016 to 2018, we collected seasonal streamwater samples from the mesocosms to quantify DIC and DOC, and we modeled the consumption of O_2 and production of DIC as zero-order kinetic reactions. We compared rates estimated from the mesocosms to rates calculated for near-stream hyporheic flow paths at an adjacent long-term well network that was sampled from 2014 to 2016. We also calculated the relative amount of hyporheic metabolism that could be explained by either the net loss of DOC or the gross inputs of stream-sourced DOC to the mesocosms. Finally, we examined the effect of season on metabolic rates and fit linear models to quantify the effects of initial streamwater DOC concentration, stream temperature, and time since packing on metabolic rates.

Study site

The study site was near the outlet of the 96-ha WS01 catchment in the H. J. Andrews Experimental Forest in the

western Cascade Mountains of Oregon, USA (44.20741 N, 122.25831 W; Fig. 1). Elevation ranged from 439 m at the outlet to 1027 m at the top of bounding ridges. The valley was deeply incised, and the slopes of the hills throughout the catchment typically exceeded 60%. The climate was marine temperate with cool, wet winters and warm, dry summers. Over the study period (water years 2014–2018), mean air temperatures at the PRIMET climate station were 9.7°C (Daly et al. 2019). December was the coldest month with mean air temperature of 1.4°C, whereas July was the warmest month with mean air temperature of 19.0°C. Over this period, mean annual precipitation was 2080 mm/y and ranged from 1783 to 2598 mm/y (Daly et al. 2019). On average, 70% of the total annual precipitation fell between November through March. Precipitation usually occurred as rain. Snow occasionally accumulated during cold winter storms, but it usually melted within several days. Over this same period, mean stream discharge at WS01 was 990 mm/y (Johnson et al. 2020). Stream flows were lowest in August with a mean of 1.3 mm/mo and highest in December with a mean of 211 mm/mo. For most of the summer, flows in the lower mainstem stream channel were spatially intermittent.

The WS01 catchment was 100% clear-cut logged between 1962 and 1966, and logging debris was burned to expose the mineral soil for reseeding Douglas-fir (*Pseudotsuga menziesii* var. *menziesii* [Mirb.] Franco). Large logs spanning the stream channel were cut, and sections blocking the channel were removed by hand. Hillslopes were replanted, and today the upland forest is a mix of 50- to 60-y-old Douglas-fir with naturally reseeded western hemlock (*Tsuga heterophylla* [Raf.] Sarg.). Red alder (*Alnus rubra* Bong.) established in the riparian zones following the harvest. Note that scientific nomenclature follows Hitchcock and Cronquist (1973).

The WS01 well network is located in a section of the valley floor that is ~14 m wide (Fig. 1) with a longitudinal gradient of 0.14 m/m. The main channel consists of series of log or boulder steps with occasional small pools. The stream bed is composed of boulders, cobbles, and gravels. The depth to bedrock within the valley appears to be shallow. The colluvial sediment averaged ~1.0 m deep and was shallower in the active channel (~0.75 m) and deeper adjacent to the bounding hillslopes (~1.30 m). A log step at the lower end of the reach failed since the well network was first established so that the lower several meters of the reach are now scoured to bedrock.

Well network

The well network, established in 1997, was composed of 34 riparian wells and 7 in-stream piezometers, arrayed in 6 transects (Fig. 1). Wells and piezometers were constructed of schedule-40 PVC pipe with an internal diameter

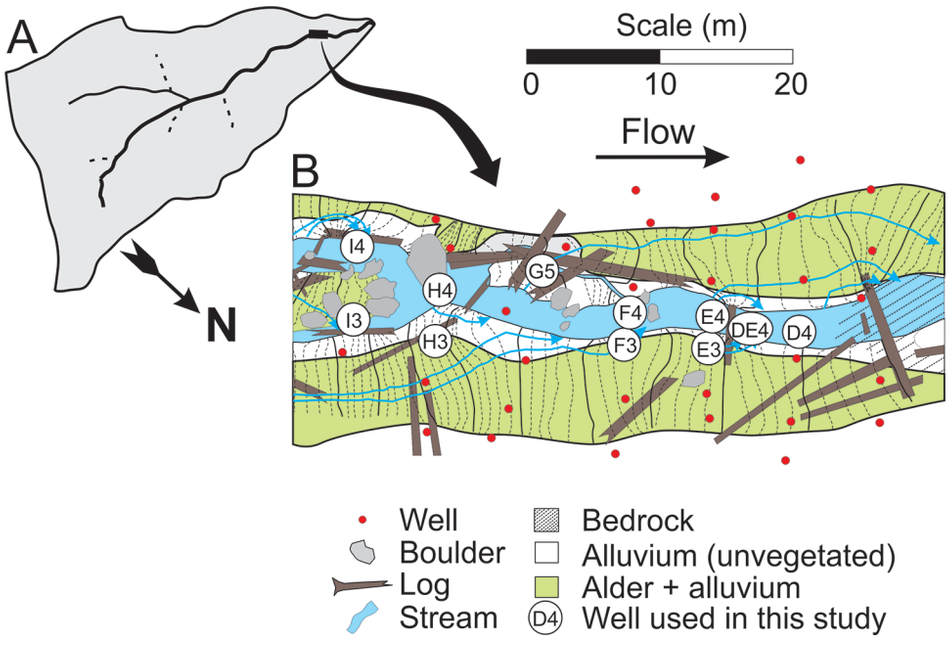

Figure 1. Location of the well network (black rectangle) within the 96-ha Watershed 1 (WS01) at the H. J. Andrews Experimental Forest in Oregon, USA. Both the mainstem and primary tributary (solid lines) are spatially intermittent in summer; dashed lines indicate ephemeral tributaries. Perennial surface flow is maintained throughout the well network reach in most summers (A). Details of the valley floor of WS01 within the well network reach and the location of individual wells used in this study. Black solid and dashed lines show simulated equipotentials (0.1-m intervals) of the water table within the valley floor. Light blue arrows illustrate some potential hyporheic flow paths through the valley floor (Kasahara and Wondzell 2003) (B). Maps are rotated so that flow through the well network reach is from left to right.

of 3.175 cm. An array of 0.32-cm diameter holes with an approximate density of 1 hole/cm^2 served as a screen along the bottom 50 cm of wells and bottom 5 cm of instream piezometers (Wondzell 2006).

The original PVC wells and piezometers were replaced with 5.08-cm internal diameter stainless steel piezometers in September 2014. The new piezometers were screened for 10 cm above a 5-cm-long drive point attached to the bottom of the casing to facilitate installation. The new piezometers were usually driven into the hole from which the PVC pipe had been removed, but in a few locations, the new piezometers were installed adjacent to the original PVC pipe. The new network consisted of 43 steel piezometers arrayed in 7 transects, including an additional transect of 3 piezometers (Fig. 1). Throughout the remainder of the manuscript, we will use wells as a general term to denote both piezometers and wells.

Pennington (2019) conducted tracer tests with salt (NaCl) at the well network site from 2014 to 2016 under a wide range of discharge conditions. Pennington used electrical conductivity (EC) breakthrough curves as a surrogate for salt concentrations, and from these he estimated median travel times of stream water to each well by using transfer function analysis. He also calculated the proportion of stream water in each well by using the ratio of the zeroth moment of each well's breakthrough curve to the zeroth moment of the corresponding stream breakthrough curve:

$$M_0 = \int EC(t)\mathrm{d}t, \qquad \text{Eq. 1}$$

where the zeroth moment, M_0, is the integral of the background-corrected EC over the duration of the tracer breakthrough curve for either the well or the stream. If the stream is well mixed and the well receives only stream water, then M_0 will be identical for the well and stream so that the resulting ratio ($M_{0\text{-stream}}$:$M_{0\text{-well}}$) will equal 1. If the well receives no tracer via stream water, then the ratio will be ~0. There are many potentially confounding factors. Wells are arrayed in transects, and for this analysis, the stream M_0 at a given transect was used as the denominator for all wells in that transect. However, tracer concentrations (NaCl, measured as EC) decreased along the length of the injection reach, and stream water reaching any well in a given transect likely enters the hyporheic zone upstream of that transect. Consequently, the zeroth moment ratio exceeded 1 in many wells. We averaged estimates of M_0 from all tracer tests for each well and selected wells with the mean zeroth moment ratio close to or >1 and median travel times ≤20 h to compare with the mesocosms. For this subset of wells, the median travel times of stream water to the wells ranged from 2.3 to 19.9 h, and the mean of the zeroth moment ratio was 1.17 and ranged from 0.85 to 2.0. See Serchan (2021) and Pennington (2019) for further details.

Hyporheic mesocosms

We constructed six 2-m-long hyporheic mesocosms, which were located on the stream bank of WS01, ~50 m downstream from the well network (Figs S1, S2). Each mesocosm consisted of two 1-m-long pipe segments connected in series. Each pipe segment was constructed from 20.3-cm internal diameter aluminum pipe sealed with high density polyethylene (HDPE) end caps. A 0.5-cm diameter hole in the center of each end cap allowed flow into and out of each segment. The bottom and top caps were identical and served to spread the point source of water at the inlet into uniform laminar flow across the full width of the mesocosm and then collapse that flow back to the outlet point, thus limiting the development of preferential flow paths and large dead zones adjacent to the end caps. To accomplish this, 18 grooves, spaced 20° apart, radiated outward from the central hole, alternating in length from 3.8, 5.7, and 8.0 cm. Each groove was narrow and shallow at the inlet hole and gradually widened and deepened along its length. A diffuser plate was placed over the grooves in the end caps to keep them free of sediment. The 20.12-cm-diameter diffuser plate was made of sintered stainless steel with high-flow square weave support layers and a nominal pore diameter of 40 μm (Porous Metal Filters, Inc, Spring, Texas).

The mesocosm segments were held vertically on an aluminum rack, and stream water was pumped to a head box >3 m above the mesocosms to provide constant head to drive flow upward through the mesocosms. Each mesocosm segment was connected with polyethylene tubing (internal diameter of 0.43 cm), first running from a main water supply pipe fed from the head box and into the bottom of the 1st mesocosm segment, and then from the top of the 1st segment to the bottom of the 2nd segment. Outflow from the top of the 2nd segment was regulated with a high precision needle valve (HOKE®, Spartanburg, South Carolina; part number 1335M4Y; Milli-mite 1300 Series valve with a globe flow pattern, in stainless steel, with a 1° stem and 0.047-inch orifice with Cv (flow coefficient) = 0.01, CRANE Instrumentation & Sampling PFT Corporation, Beijing, China). The total flow path from the inlet of the 1st mesocosm segment to the outlet of the 2nd segment defined a 2-m hyporheic flow path. We assumed that the tubing connecting the segments of each mesocosm had minimal influence on biogeochemical processing compared with the combined length of the 2 pipe segments because of the tubing's limited surface area and short residence times.

We maintained flow rates through each mesocosm as close to 48 mL/min as was possible throughout the duration of the study (May 2016–Sept 2018). We measured flow velocities with tracer tests showing that median travel times through the 2-m mesocosms ranged from 9.12 to 13.87 h (mean = 10.43 h, σ = 1.06 h) across all mesocosms on all sample dates. Thus, with a flow rate of 48 mL/min, the

mean flow velocity through the mesocosms was 0.19 m/h and ranged from a low of 0.18 m/h to a high of 0.21 m/h, which closely matched flow velocities observed in the well network during tracer tests.

We collected the sediment used to pack the mesocosm segments from the bedload trap basin located at the mouth of the WS01 catchment, ~150 m downstream from the well network. The basin sorts sediment, with the coarsest bedload being dropped at the head of the basin and the finest sediment and most organic matter accumulating in the deepest and most distal end of the basin. We chose a location about $^1/_3$ of the distance along the length of the basin, where surface sediment was dominated by fine gravel, sand, and finer textured mineral sediment but with little to no obvious accumulation of organics. In August 2014, the bedload trap basin was drained and allowed to dry for several days. After this drying period, we dug moist sediment from the floor of the basin and sieved it through galvanized wire mesh with square openings measuring ~6 mm (1/4 inch) on a side to remove all large particles. Standing water was not present over the excavated material, so fines were not washed from the sediment as it was dug and sieved. After sieving, we transferred the sediment to woven polypropylene sandbags, which we then layered along the upstream face of the dam so that they would be underwater once the catch basin was refilled a few days later. The sediment was thus stored under water until we were ready to pack the mesocosms.

We packed the mesocosms in May 2016. We first retrieved sandbags from the pond and allowed them to drain by gravity. The woven polypropylene material is relatively tight, so the sandbags drained slowly with little loss of fine materials. To ensure homogeneity during packing, we emptied 2 to 3 sandbags into a plastic tub and mixed them with a shovel. Then we dumped a small scoop of sediment (~500 g) into each of the 12 mesocosm segments. A 2nd scoop was added to each of the 12 segments, and the mesocosms were ultimately filled by continually adding scoops in sequence. This sequential packing was intended to spread any variation in sediment texture or organic matter content evenly across all 12 pipe segments. Once the tub was empty, we used a long-handled square point tamper (10.16 cm × 10.16 cm) to compact the layer of sediment in each pipe. Then, we refilled the tub with sediment and repeated these steps until all 12 pipe segments were full. In total, 24 sandbags of sediment were needed to pack all 12 pipe segments.

We compared the size class fractions and organic C content of the sediment used to pack the mesocosms with sediment from the streambed and streambanks in the stream reach with the well network. We collected 39 samples from the stream and 29 samples from the sieved sediment for the mesocosms. Sediment was oven dried (105°C for 24 h), weighed, and split into 2 parts. We sieved ½ of the sample (φ -3 to 5) for sediment size-class analysis (Folk 1974). The other ½ of the sample was again oven dried (105°C for 24 h) and then weighed immediately after removing from the oven. The sample was then combusted in a muffle furnace (450°C for 5 h) after which it was immediately reweighed to measure mass loss on ignition. We used a conversion factor of 0.55 (Hoogsteen et al. 2015) to convert combustible sediment organic matter into organic C. We then visually compared plots of the cumulative proportion of sediment size-class fractions (Fig. S3A) and organic C content (Fig. S3B) for the sediment used to pack the mesocosms and sediment sampled from the stream bed and banks to confirm that they were similar.

The mesocosms were enclosed in an insulated aluminum box in an attempt to maintain field-like hyporheic temperature. We continuously circulated stream water in ~18 m of soft copper tubing (9-mm outside diameter), which we coiled to make radiators. We placed radiators between 2 pipe segments because it would have been logistically impossible to wrap each pipe segment in copper coil. We placed 2 electric heat cables with built-in thermostat inside the enclosures to prevent freezing in winter months.

We installed a filter system to prevent clogging of the sintered stainless-steel diffuser plates, which had a nominal pore diameter of 40 μm. We pumped stream water through a 500-μm filter and then a 150-μm filter to the head box located >3 m above the main influent line to the mesocosms. We routed water from the head box through polyethylene tubing to a final 50-μm filter and from there to the main feed line to the mesocosms. The filters may have kept some particulate organic matter (POM) from entering the mesocosms, but this effect is likely small for 2 reasons. First, comparison of filtered vs unfiltered water by Corson-Rikert et al. (2016) showed that little POC was present in stream water under winter (high) baseflow conditions. Second, the size of POM exported by streams at the H. J. Andrews tends to be small, averaging 3 to 12 μm in diameter with ~80% of POM ranging in size from 0.45 to 53.0 μm (Naiman and Sedell 1979). Consequently, most of the POM transported in WS01 should easily pass through our filter system.

Stream water has flowed through the mesocosms continuously since May 2016. A few notable exceptions include short periods when filters clogged after large storms, when equipment broke down, or when power outages occurred. We monitored the flow and corrected problems as soon as possible after they occurred. Except for our 1st sample in October 2016, water sampling only occurred if flows through the mesocosms had been uninterrupted for at least 6 wk. Unfortunately, the water supply system became clogged with sediment and coarse organic material during a storm just before our 1st planned sample. Flow through the mesocosms stopped at 16:50 on 19 October 2016. We restored flow at 17:00 on 22 October, and immediately afterward, dissolved O_2 concentrations in the outlet water fell to a

minimum of 0.01 mM. Over the next 24 h, dissolved O_2 at the mesocosm outlets gradually recovered to the pre-storm concentrations. We sampled the mesocosm outlets on 23 October between 16:00 and 17:00 when the outlet dissolved O_2 was 97% of the pre-storm mean concentration. Dissolved O_2 concentrations peaked around midnight between 23 and 24 October at 0.25 mM, or 102% of the pre-storm mean.

The mesocosms were instrumented with a variety of in-line sensors to provide real time monitoring. The main water supply line was split into 3 sub-lines, each feeding a pair of mesocosms. Each of the 3 sub-lines included an in-line EC sensor (CS547A-L, Campbell Scientific®, Logan, Utah), a venturi mixer (6.4-mm Venturi Injector, A2Z Ozone®, Louisville, Kentucky), and an injection port. In-line EC sensors were also located at the outlet of all 6 mesocosms along with an electronic flow meter to monitor flow rates in real time. Sampling ports were located on the inlet tube to each individual mesocosm, between the 2 segments of the mesocosm, and at the outlet from the 2nd segment.

Field sampling and laboratory analyses for DIC and DOC

Laboratory work was completed at the Institute for Water and Watersheds Cooperative Chemical Analytical Laboratory (CCAL) in Corvallis, Oregon. Prior to field work, all laboratory and field sampling equipment, including 250-mL HDPE bottles, TraceClean® 40-mL borosilicate vials (VWR®, Radnor, Pennsylvania), 60-mL syringes with Luer-Lok™ tips (Becton, Dickinson and Company, Franklin Lakes, New Jersey), Masterflex® fitting polycarbonate stopcocks with luer connections (item# SK- 30600-03; Cole-Parmer, Vernon Hills, Illinois), polypropylene filter holder for 47-mm filter (item# UX-06623- 22; Advantec MFS, Inc., Dublin, California), and sample tubing (outer diameter = 0.635 cm) were rinsed in deionized water, soaked in a 10% v/v HCl acid-bath solution overnight, re-rinsed and soaked in deionized water, and air dried in a fume hood. We further processed the borosilicate vials for DOC analysis by combusting them in a muffle furnace at 550°C for 3 h. After the vials cooled, we stored them in air-tight containers. We rinsed the 47-mm GF/F glass microfiber filters in 1 L of deionized water and dried them overnight in a drying oven at 70 to 80°C. We then placed each filter paper in an aluminum foil packet (~5 cm × ~5 cm), which we combusted in a muffle furnace at 550°C for 3 h. After cooling, we sealed the aluminum foil packets and stored in air-tight clean Ziploc® (SC Johnson, Racine, Wisconsin) bags (CCAL 2013).

Sampling the well network We sampled wells at roughly monthly intervals, from July 2014 to June 2015 and on 3 separate occasions in 2016 (Fig. 2). The first 2 samples in 2014 were from the original PVC well network, and all subsequent samples were collected from the new stainless-steel well network. Sampling the well network took 2 d. On the 1st day, we measured water elevation, pH (YSI Model 60 pH meter, Yellow Springs Instruments, Yellow Springs, Ohio), temperature and dissolved O_2 (YSI ProODO dissolved O_2 meter, Yellow Springs Instruments, Yellow Springs, Ohio) and EC (WTW ProfiLine Cond 3110 portable conductivity meter, Xylem Analytics, Weilheim Germany). We then purged the wells by pumping until they

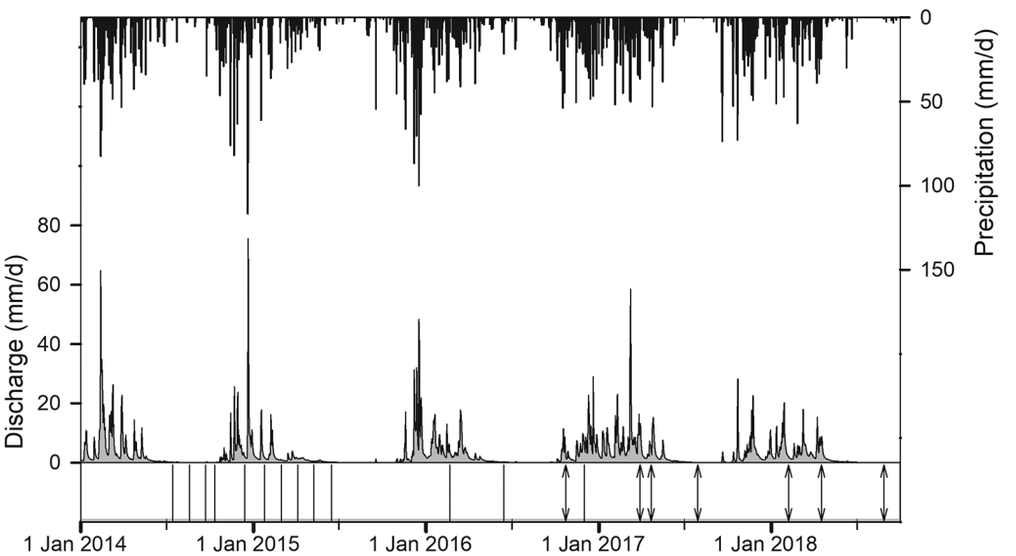

Figure 2. Stream discharge (Johnson et al. 2020) and precipitation (Daly et al. 2019) over the study period for Watershed 1 at the H. J. Andrews Experimental Forest in Oregon, USA. Vertical lines indicate well network sampling dates and vertical double-ended arrows indicate mesocosm sampling dates.

were dry or until a volume of ~700 mL of water had been removed from the well (equivalent to ~35 cm of water in the well). We collected water samples the following day after the wells refilled. Before sampling, we rinsed all sampling equipment twice with well water. After rinsing, we collected a filtered sample (Whatman GF/F microfiber glass filter), filling a 250-mL HDPE bottle. Then we collected a 60-mL sample of unfiltered water in a syringe, after which we immediately closed the valve to isolate the water sample from the air. Note that the field-filter apparatus and the sample tubing were reused after rinsing with well water from the next sample location. We used the same technique to collect filtered and unfiltered streamwater samples. We stored samples in an ice chest kept cold with ice packs and then transported them to the lab where they were refrigerated at 4°C until analyzed.

Sampling the hyporheic mesocosms We sampled the mesocosms through ports located at the inlet, mid-point, and outlet, representing measurements taken at 0.0, 1.0, and 2.0-m along hyporheic flow paths. To collect a sample, we stopped flow downstream of the sample port by closing a valve, and we opened the sample port so that the sample collection rate was close to 48 mL/min—the same rate as the flow through each mesocosm to minimize the potential to develop preferential flow paths through the sediment when sampling. We measured dissolved O_2 and temperature in an ~15-mL flow-through cell containing the probe end of a YSI ProODO dissolved O_2 meter. We measured pH and EC in ~20 mL of water collected in a graduated cylinder. We then attached a 60-mL syringe to the sampling port to collect the water sample, following the sampling methods described above for the well network. We first used the syringe to collect a 250-mL filtered sample in an HDPE bottle. Then we filled the syringe to collect a 60-mL unfiltered sample, after which we closed the valve to isolate the water sample from the air. We collected field duplicates from both the stream and mesocosms for quality assurance.

Before February of 2018, we sampled all 6 inlet ports, then the intermediate ports, and finally the outlet ports. Sampling required 0.5 to 1 h at each location (~3 h total sampling time), whereas the mean travel time through 2-m mesocosms was 10.43 h. We modified our sampling protocols to support characterization of changes in parcels of water moving through the mesocosms (i.e., Lagrangian sampling) starting in February 2018. First, we intentionally timed rounds of sampling to coincide with the travel time of water flowing through the mesocosms, waiting 5 to 6 h to sample the intermediate ports and another 5 to 6 h to sample the outlets. Second, to reduce the time needed to collect field samples, we designed a sampling system that consisted of 3 sets of 6 acid-washed sample bottles (500-mL HDPE Nalgene®; Nalge Nunc International Corp., Rochester, New York). We used each set of bottles to collect water from the 6 inlet, intermediate, and outlet ports. A set of 6 sample bottles would be connected to 6 sampling ports to collect ~500 mL of unfiltered water, regulating the flow rate to ~48 mL/min by using the valve on the sample port. The 500-mL sample bottles were rigged with inlet and outlet tubes that fit tightly into holes drilled into the bottle caps to minimize chances for contamination when collecting the water sample. The actual water sample was then collected using a 60-mL syringe connected to the outlet tube of the 500-mL bottle rather than directly to each mesocosm's sampling port. See Serchan (2021) for additional details.

Laboratory analyses for DIC and DOC All laboratory analyses followed CCAL's standard operating procedures. Detailed descriptions of the methods and references to the procedures are given in Serchan (2021). Briefly, both DIC and DOC were analyzed on a TOC-VCSH combustion C analyzer (Shimadzu, Kyoto, Japan). Samples were analyzed for DIC within 24 hours and for DOC within 72 hours.

Data analyses

We compared concentrations, C_i, of each selected i-th constituent, O_2, DIC, and DOC (mM), with travel time through both the well network and through the mesocosms. For both the well network and the mesocosms, we modeled the consumption of O_2 and production of DIC as zero-order kinetic reactions with O_2 consumption rate (k_{O2}) and DIC production rate (k_{DIC}). We used zero-order kinetics because plots of C_i vs travel time were approximately linear (see Fig. 3). Also, 1st-order kinetics are not appropriate to describe the accumulation of a product from a reaction because the rate is dependent on the concentration of the reactant at time 0. Thus, we used simple linear regression (Proc REG, SAS® version 9.4; SAS Institute, Cary, North Carolina) and treated the slope of the regression line as the rate, k_i (mM/h):

$$C_i(t) = b + k_i \times \bar{t}, \qquad \text{Eq. 2}$$

where C_i is the concentration, b is the intercept, k_i is the slope, and $\bar{t}$ is either the median travel time for stream water to reach a well or the median travel time through the mesocosms (in h). Note that the k_i values from the mesocosms and well network datasets are not perfectly comparable. In the mesocosms, the changes in solute concentrations are measured at 0, 1, and 2 m along 6 individual, isolated but replicated flow paths. The values estimated from the well network come from wells with varying travel times, and each well captures a unique set of flow paths along which stream water flows, thus allowing much greater potential for spatial heterogeneity in process rates.

We examined the influence of inlet DOC concentrations, water temperature, time since packing, and season of year as possible controls on respiration rates, k_{O2} and k_{DIC}. We

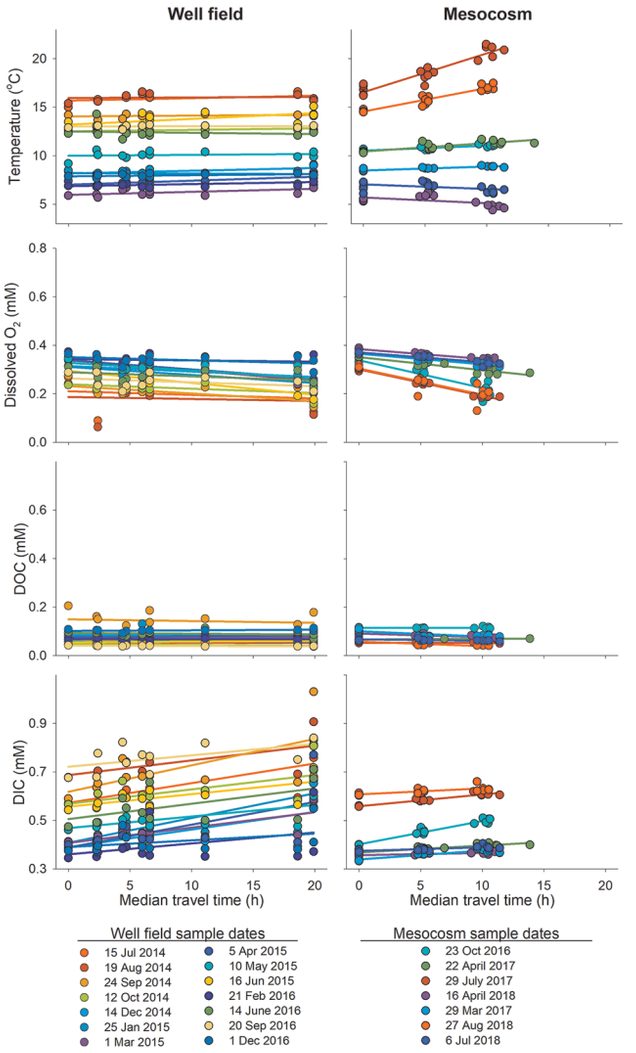

Figure 3. Patterns of water temperature, dissolved O_2, dissolved organic C (DOC), and dissolved inorganic C (DIC) vs median travel time for the well field and the mesocosms at the H. J. Andrews Experimental Forest in Oregon, USA. Colors denote approximate water temperature at the time of sampling: reds are warmest, and blues and purples are coldest.

sampled the mesocosms only 7 times, which was not sufficient to characterize all 4 seasons. Thus, we grouped samples from July, August, and October as summer–autumn because they were collected during low-flow periods and during the growing season or leaf fall, although the October sample was collected at the tail end of the 1st autumn storm. We collected the winter–spring samples during February, March, and April, in the middle of or late in the rainy season when stream flows were higher and when water temperatures were cooler. Statistical approaches to data analysis were limited because of the small sample sizes, the potential for autocorrelation given the repeated measures sampling in both the mesocosms and well network, and lack of independence among our predictor variables. Therefore, we used only simple descriptive statistics. Specifically, we examined relationships among inlet DOC concentrations and water temperature, and in the mesocosm, time since packing, with k_{O2} and k_{DIC} as measured in either the mesocosms or well network using simple linear regression. We used a 2-tailed t-test for independent means to compare mean k_{O2} and k_{DIC}, both between seasons and between the mesocosm and the well field, calculating the effect sizes for the differences between the means as Cohen's d.

We also examined the mesocosm data to estimate the relative amount of the hyporheic metabolism that could be explained by the net loss of DOC. To do this, we calculated the change in concentration measured at the outlet minus those at the inlets ($\Delta C_i = C_{i,out} - C_{i,in}$), where positive ΔC_i indicates production and negative ΔC_i indicates consumption. We assumed that aerobic respiration was the only process that utilized O_2 and produced DIC along the hyporheic flow paths through the mesocosms, thus ignoring other processes that could influence ΔC_{O2} and ΔC_{DIC}. Given this assumption, we examined if 1) the observed net loss of DOC or 2) the total amount of stream-sourced DOC could account for the observed loss of O_2 and gain of DIC. We assumed a 1:1 stoichiometric relationship for C metabolism, i.e., that 1 mol of DOC accounts for consumption of 1 mol of O_2 and production of 1 mol of DIC, as has often been done elsewhere (Findlay et al. 1993, Findlay and Sobczak 1996, Battin et al. 2003, Mermillod-Blondin et al. 2005). Clearly, this is a simplification because DOC compounds in the mesocosms and the hyporheic zone of the well field would be composed of a diversity of compounds with varying stoichiometries. Finally, in 12 out of 42 cases, ΔDOC was positive, though small, potentially suggesting modest production of DOC along hyporheic flow paths. The largest increase in DOC was 0.0058 mM and the mean increase was 0.0027 mM. For comparison, the mean difference between 77 samples and their co-collected field duplicates was 0.0037 mM (note: a total of 456 samples were collected along with an additional 77 field duplicates). Because the increases in DOC were small relative to sample error, we are unsure if these are real changes. However, we kept the increases in ΔDOC (i.e., did not set them to 0) in our analyses, except when calculating the proportion of ΔO_2 and ΔDIC that could be accounted for by the observed net change in DOC, which we set to 0 in these cases.

RESULTS

Comparison between wells and mesocosms

We sampled the well network 14 times between July 2014 and December 2016 and the mesocosms 7 times between October 2016 and August 2018 (Fig. 2). Our sampling strategy targeted baseflow or near-baseflow conditions, but this was not always possible, especially during the

winter rainy season. Stream discharge ranged from 0.169 to 838.5 L/s over the duration of our study, whereas we collected samples at discharge ranging from 0.5 to 123.7 L/s. Although the sampling periods for the well network and the mesocosms mostly did not overlap, sampling did occur during similar seasonal weather and flow conditions, allowing reasonable comparisons to assess whether the mesocosms represented actual hyporheic flowpaths. Specifically, we examined changes in temperature, dissolved O_2, DIC, and DOC along flow paths through the mesocosms, and contrasted those to the changes observed between the stream and wells dominated by stream-sourced water and with median travel times (<20 h) similar to those of the mesocosms (10.4 h).

Temperature changes along hyporheic flow paths in the well network were similar to those in the mesocosms except during the hottest sample dates during the summer (Fig. 3). Temperatures were similar among all wells in the well network on each sample date and reflected the streamwater temperature, regardless of travel time. A similar pattern was observed in the mesocosms during winter–spring, when air and streamwater temperatures were cool. However, during the summer when air temperatures were hot, water temperature increased with travel time through the mesocosms. The mesocosms' insulation and radiator were insufficient to prevent warming when air temperatures were very hot so that internal mesocosm temperatures increased by as much as 5°C, from inlets to outlets, during the warmest sampling dates.

In general, dissolved O_2 in the stream water was near saturation. The O_2 concentrations were greater in winter when stream temperatures were cooler than in summer when temperatures were warmer (Fig. 3). Streamwater DOC concentrations were also higher in winter–spring than in summer–autumn, whereas DIC concentrations were higher in the summer–autumn than in winter–spring. We tended to see declines in dissolved O_2 concentrations with distance through the mesocosms, especially when water warmed. This change in O_2, however, was not due to supersaturation of O_2 and degassing with increasing temperatures and decreasing solubility. O_2 saturation is also a function of pressure and, with head in excess of 3 m of H_2O at mesocosm outlets, water in the mesocosms never reached O_2 saturation. For example, in the worst-case scenario when the water warmed by ~5°C on 29 July 2017, pressurizing the water and warming would have resulted in 86.1% saturation at the mesocosm outlets (assuming no change in the actual concentration of dissolved O_2). More generally, once water was pressurized, the O_2 saturations ranged from 83.8% to 72.0% at the inlets and from 72.6% to 17.4% at the outlets, at the observed pressure, temperatures, and salinity.

The overall changes in concentrations of dissolved O_2, DOC, and DIC along hyporheic flow paths showed similar direction in trends in both the well network and the mesocosms (Fig. 3). In general, concentrations of dissolved O_2 decreased with travel time and concentrations of DIC increased, whereas there was little net change in DOC. Net decreases in DOC were much smaller than the observed increase in DIC on most sample dates, in both the well network and the mesocosms. Although the direction of trends was generally similar between the well network and mesocosms, the absolute magnitude of the changes was different (Fig. 3).

During the summer–autumn the mean k_{O2} was 4.67 standard deviations (SD) higher in the mesocosms than in the well network ($p < 0.001$; Cohen's $d = 4.67$; Fig. 4A). The mean k_{O2} was also higher in the mesocosms in the winter–spring, but the effect size was smaller ($p < 0.001$; Cohen's

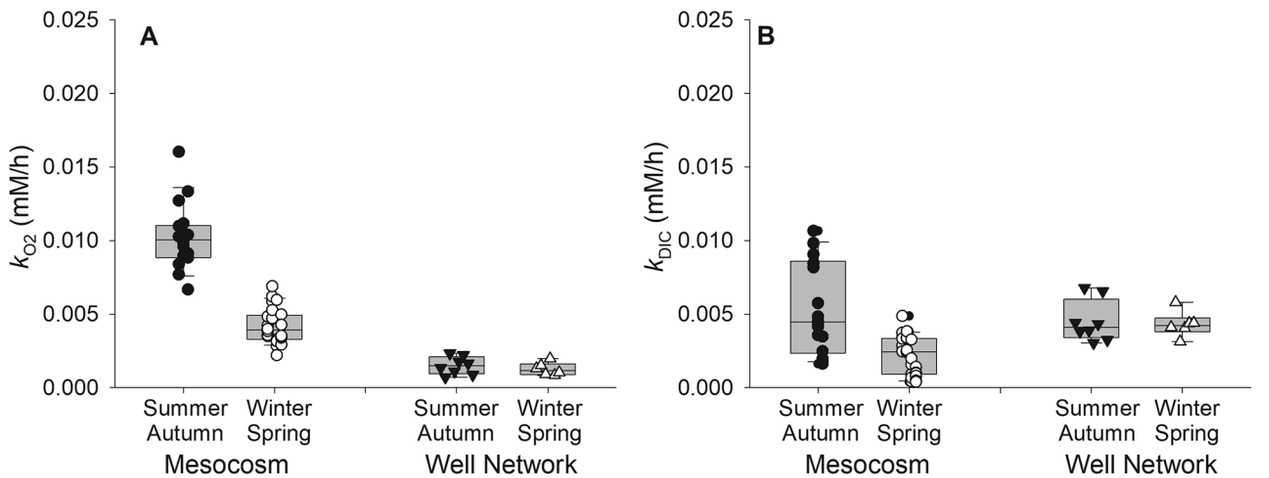

Figure 4. Comparison of zero-order reaction rates for the consumption of dissolved O_2 (k_{O2}) (A) and the production of dissolved inorganic C (k_{DIC}) (B) between the mesocosms and the well network and between seasons (summer–autumn and winter–spring) at the H. J. Andrews Experimental Forest in Oregon, USA. Data points (circles and triangles) for all individual measurements are plotted on top of box and whisker graphs showing the median, quartiles, and the 10th and 90th percentiles (whiskers).

d = 2.66; Fig. 4A). The mesocosms also showed strong seasonal differences in mean k_{O2} ($p < 0.001$; Cohen's d = 3.56; Fig. 4A), whereas seasonal differences in mean k_{O2} were not evident in the well network ($p = 0.41$). During summer–autumn, the range in k_{DIC} was larger in the mesocosms than in the well network, although the mean rates were not different ($p = 0.37$; Fig. 4B). In the winter–spring, the mean k_{DIC} was 1.72 SD larger in the well network than in the mesocosms ($p < 0.003$; Cohen's d = 1.72; Fig. 4B). The mesocosms also showed seasonal differences in mean k_{DIC} ($p < 0.001$; Cohen's d = 1.39; Fig. 4B) whereas there were not seasonal differences in the well network (p = 0.75).

Factors controlling metabolism in the mesocosms

We expected that the factors strongly related to k_{O2} would also be strongly related to k_{DIC} because the changes in O_2 and DIC are related, at least in part, through heterotrophic respiration. However, k_{O2} and k_{DIC} only showed similar patterns with temperature, in both cases showing positive significant trends in the mesocosms (Figs 5 and 6). However, this relationship was weak for k_{DIC} (r^2 = 0.10), and the slope was ~3× steeper for k_{O2} than for k_{DIC}.

The k_{O2} was not related to the inlet DOC concentrations in either the mesocosms or the well network, nor was the k_{O2} related to time since packing in the mesocosms (Fig. 5). In contrast, the k_{DIC} was weakly related to inlet DOC concentration in both the mesocosms and the wells (r^2 = 0.22 and 0.26, respectively; Fig. 6). The trend towards increasing k_{DIC} with increasing stream DOC concentrations in the mesocosms was strongly leveraged by a single sample date on which stream DOC was unusually high. Finally, k_{DIC} was strongly related to the time since the mesocosms were packed (Fig. 6).

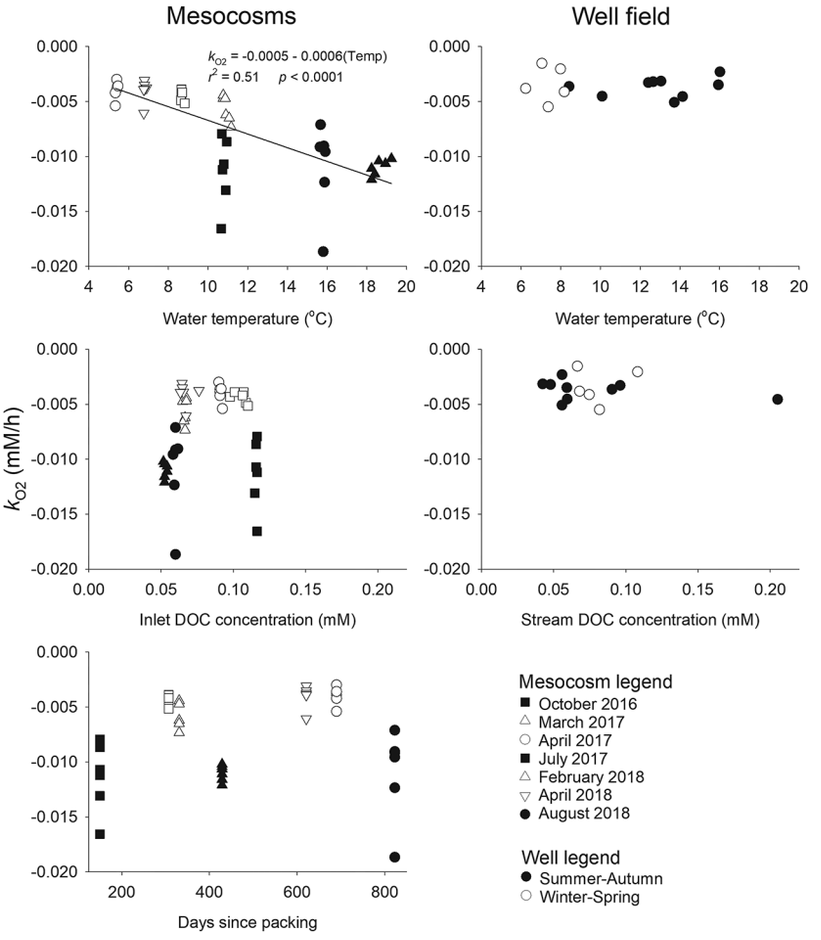

Figure 5. Comparison of factors controlling the rate of dissolved O_2 consumption (k_{O2}) in the mesocosms and the wells at the H. J. Andrews Experimental Forest in Oregon, USA. Black-filled symbols represent summer–autumn samples, and white-filled symbols represent winter–spring. Six replicates are reported from the mesocosms on each of the 7 sample dates, whereas only a single k_{O2} could be calculated from the well network on each of the 14 sample dates. Regressions are shown if slopes were different from 0 ($p < 0.1$).

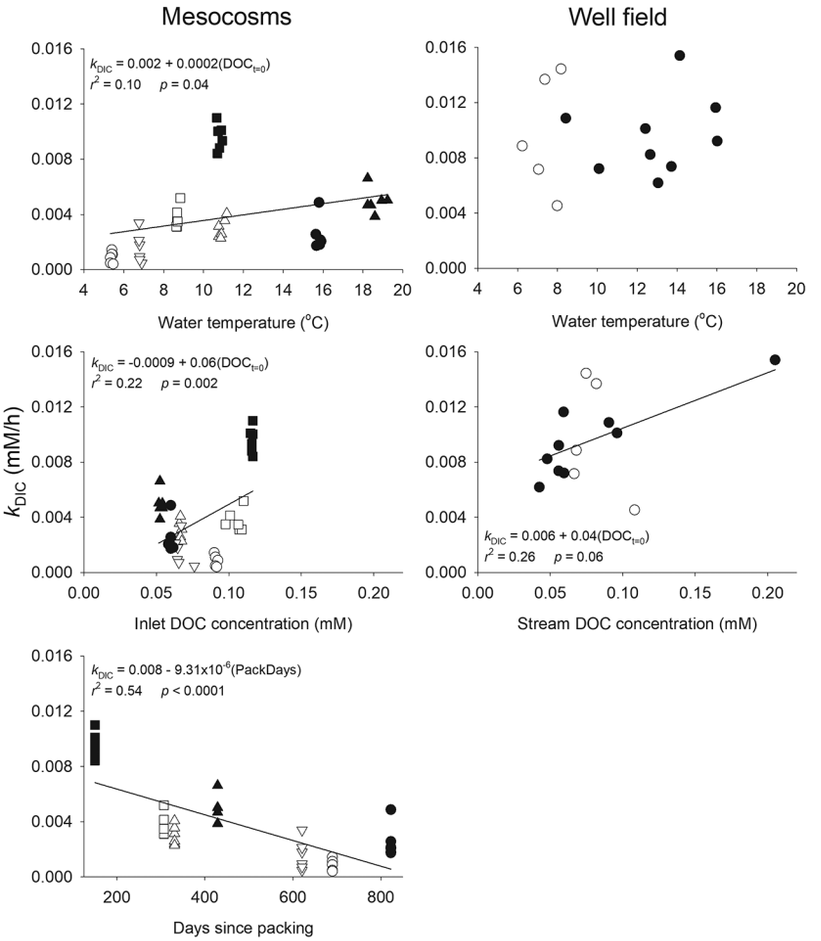

Figure 6. Comparison of factors controlling the rate of dissolved inorganic C production (k_{DIC}) in the mesocosms and the wells at the H. J. Andrews Experimental Forest in Oregon, USA. Black-filled symbols represent summer–autumn samples, and white-filled symbols represent winter–spring. Six replicates are reported from the mesocosms on each of the 7 sample dates, whereas only a single k_{DIC} could be calculated from the well network on each of the 14 sample dates. Regressions are shown if slopes were different from 0 ($p < 0.1$). Symbols follow legend in Fig. 6.

Net changes in dissolved O_2, DOC, and DIC within the mesocosms

Because the mesocosms are closed systems for which there is no mixing of water and solutes from other sources, net changes in dissolved O_2, DOC, and DIC between the inlets and outlets can only occur because of biogeochemical reactions within the mesocosms. The ΔO_2 concentration from the inlets to the outlets averaged –0.076 mM over all sample periods (SD = 0.04, range –0.179 mM to –0.033 mM) and ΔDIC averaged 0.0388 mM, (SD = 0.029, range 0.004 mM to 0.111 mM), whereas the net ΔDOC was an order of magnitude smaller, averaging only –0.008 mM (SD = 0.010, range –0.030 mM to 0.006 mM). For all sampling dates, the amount of O_2 utilized was at least 2× greater than the net change in DOC. There were seasonal differences in the magnitudes of both ΔO_2 and ΔDIC ($p < 0.001$; Fig. 7), where the magnitudes in summer–autumn were greater than the magnitudes in winter–spring. However, the magnitudes of ΔDOC did not display seasonal differences ($p = 0.312$; Fig. 7).

The O_2 losses and DIC gains observed across the mesocosms are difficult to relate to the source of organic C for aerobic metabolism. If these are examined on the basis of gross streamwater inputs of DOC, then input DOC could completely account for the ΔO_2 and ΔDIC observed in the winter–spring, assuming a 1:1 stoichiometric relationship. In the summer–autumn period however, complete utilization of all input DOC would account for only 71% of the observed net loss of O_2. And during extreme low-flow periods in late summer, inputs of DOC could only account for 53% of the observed loss of O_2. The ΔO_2 and ΔDIC can also be compared with the observed net losses of DOC. In this case, ΔDOC accounted for as little as 0% to as much as 59% of the ΔO_2, with an overall mean of 17%. There were also strong seasonal differences in the percentage of O_2 that could be explained by the net loss

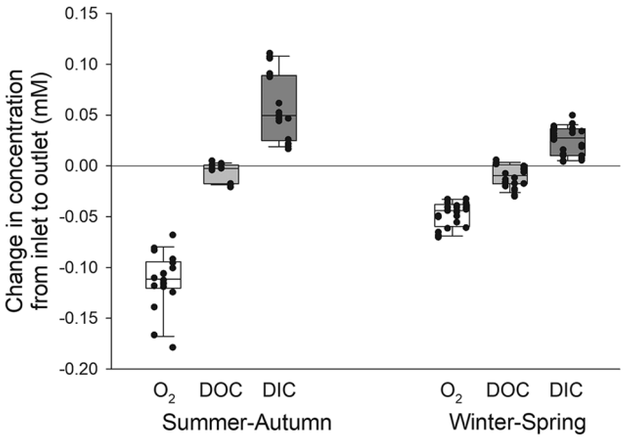

Figure 7. Change in concentration of dissolved O_2 (ΔO_2), stream-sourced dissolved organic C (ΔDOC) and dissolved inorganic C (ΔDIC) along 2-m-long flow paths through the hyporheic mesocosms, contrasting the summer–autumn and winter–spring seasons at the H. J. Andrews Experimental Forest in Oregon, USA. Negative values indicate consumption, whereas positive values indicate production. Bars show the median and 25th and 75th percentiles; whiskers show the 10th and 90th percentiles. The data from each mesocosm is plotted over the boxplot. Points are jittered along the *x*-axis to separate each sampling date.

of DOC ($p = 0.0019$). On average, only 7% of O_2 loss could be explained by net loss of DOC in summer–autumn compared with 24% of the O_2 loss in winter–spring. Similarly, the percent DIC produced from the net loss of DOC also differed seasonally ($p = 0.03$). On average, 29% of DIC gains could be explained by the net loss of DOC in summer–autumn compared with 77% of the DIC gains in winter–spring with an overall mean of 56% of DIC explained by the net losses of DOC.

DISCUSSION

The mesocosms provided reasonable simulations of the variation in hyporheic respiration observed in the well field along this steep, mountainous headwater stream. Both changes in solute concentrations with travel time through the hyporheic zone and the direction of trends estimated in the consumption of O_2 and production of DIC were similar in the well field and the mesocosms. The mesocosm results, showing that aerobic metabolism of stream-sourced DOC was insufficient to account for concurrent decline in O_2 and increase in DIC along hyporheic flow paths, confirmed results of previous well-field studies hypothesizing that sediment-bound or buried POC was the predominant source of organic C for hyporheic respiration in this stream. DOC from autochthonously produced organic C has long been considered more bioavailable than DOC from allochthonous sources, so that stream-sourced DOC is thought to be relatively less important to the metabolism of heavily shaded forest streams. Our results suggest other factors are also important, especially the amount of hyporheic exchange. In summer and autumn, when discharge was so low that all the stream water was exchanged through the hyporheic zone over channel distances of 100 m or less, hyporheic exchange likely stripped most of the bioavailable DOC from the stream water and provided little opportunity for new, relatively bioavailable DOC to accumulate. In the winter and spring, however, water temperatures and respiration rates were lower, and discharge was higher so that hyporheic turnover lengths were longer. Further, DOC leached from relatively fresh allochthonous organic matter stored in the channel after leaf and needle fall in autumn, or DOC inputs from groundwater during the winter wet season, resulted in higher DOC concentrations in stream water. Thus, hyporheic respiratory demands were lower, and bioavailable DOC may have been more abundant such that stream-sourced DOC was relatively more important in winter-spring than in summer and autumn. Importantly, decreases in O_2 and increases in DIC along flow paths through the mesocosms were linear when plotted against travel time. This pattern suggests that the processes that generate bioavailable DOC from sediment-bound and buried POC control the rates of aerobic respiration in the hyporheic zone in this stream.

Do the mesocosms represent the hyporheic zone?

The age of deposited sediment may help explain observed differences in hyporheic community respiration rates (k_{O2}) between the mesocosms and the well network. The valley-floor colluvium in WS01 was most likely deposited in the runout zones of debris flows. Debris flow deposits have been emplaced in recent decades in several nearby catchments, where key pieces of large wood wedge across the narrow valleys, forming log jams with colluvial deposits stretching long distances upstream (Nakamura and Swanson 1993). We do not know the age of the colluvium in the valley floor of the well network reach of WS01, but debris flows have not occurred since the watershed was first instrumented for a paired-watershed study in 1952. In contrast, the mesocosms were packed in 2016 with sediment eroded from the catchment in the winter of 2013 to 2014. The samples for size class distributions and organic matter content suggest that the mesocosm sediment is similar to that of the immediate streambed and banks. However, these samples were collected within a few 10s of cm from the active channel in locations potentially influenced by deposition of new organic matter. We do not have sediment samples from the well network reach from locations further into the hyporheic zone that would be more isolated from surface processes. Thus, our sediment samples, collected from the streambed and stream banks, may not accurately reflect processes occurring within the well network, which extends many meters from the stream and can capture the influence of hyporheic flow paths > 10 m long.

Because both the wells and mesocosms receive the same stream-sourced DOC, the differences we observed in metabolic activity suggest that the microbial availability of the sediment-bound or buried organic C might be quite different between the mesocosm sediment and that of the valley floor. The mesocosm k_{DIC} showed a strong packing effect, with the highest rates of DIC production observed on the 1st sample date in October 2016, even though 5 mo had elapsed between the date on which the mesocosms were packed and that 1st sample. This relationship was not observed for k_{O2}, perhaps because the composition or bioavailability of the sediment-bound or buried POC changed over time, as suggested by a clear decreasing trend in the respiratory quotient (calculated as the ratio of $|\Delta DIC|$ to $|\Delta O_2|$) from October 2016 to August 2018 (Fig. 8). These results have important implications for short-term laboratory column experiments or other mesocosm experiments using native sediment because the disturbance of packing might enhance metabolic activity if measurements or experiments are conducted in the 1st few years after packing with sediment.

Direct comparison between the mesocosms and the near-stream hyporheic flow paths pointed to other differences between these 2 systems. For example, the change in water temperature with travel time was often much greater in the mesocosms than in the well network. However, the mesocosms are located above ground, and even though they are in an insulated enclosure, we were unable to prevent temperature changes along flow paths through the mesocosms when the air temperature was greatly different than the stream temperature. This was mostly a problem on warm summer days, and k_{O2} was much higher in the summer in the mesocosms than in the well network. Further, the direct comparisons between the rates and water temperature in the mesocosms showed increases in both k_{O2} and k_{DIC} as temperatures warmed.

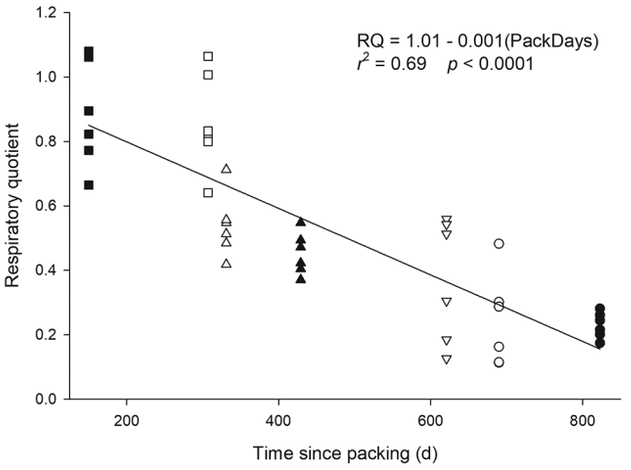

Figure 8. Respiratory quotient (RQ = $|\Delta DIC|$ / $|\Delta O_2|$) over time since packing the mesocosms (PackDays). Symbols follow those for the mesocosm shown in legend for Fig. 6.

The rates for both k_{O2} and k_{DIC} were lower in winter–spring than in summer–autumn in the mesocosms, but there was little difference between seasons in the well network. It seems unlikely that differences in the concentration or quality of DOC in the stream water can explain this difference because both the mesocosms and the wells received the same stream-sourced water. Thus, the seasonal differences in the mesocosms are likely related to differences in organic C availability interacting with seasonal differences in temperature.

Although the mesocosms differed from the well network for several of the metrics we examined, these differences may be explained by differences in time since sediment disturbance (packing) and temperature in the mesocosms. Thus, although the mesocosms do not exactly replicate in situ processes in the hyporheic zone, they do provide a reasonable platform to further explore the biogeochemical processing of organic C in the hyporheic zone of WS01.

Factors controlling metabolism in the mesocosms

The utilization of O_2 and DOC and the accumulation of DIC are often tightly coupled through microbial respiration in aerobic zones within the hyporheic zone. Thus, fitting a zero-order kinetic model to the change in O_2 concentrations with travel time provides an estimate of the underlying hyporheic community respiration rate. Hyporheic respiration varied seasonally, with mean summer–autumn k_{O2} approximately twice as large as winter–spring k_{O2}. A similar trend was observed for k_{DIC}. However, season is a complex categorical variable that likely includes effects of changing water temperature, changing concentrations of DOC, and changes in the proportion of stream water that has already cycled through the hyporheic zone, all of which are likely to influence the bioavailability of DOC. We expected that comparisons of respiration rates with stream temperature, DOC concentrations, and time since packing would be similar for both k_{O2} and k_{DIC}. That was not the case, with k_{O2} only correlated to water temperature but k_{DIC} correlated to water temperature, inlet DOC concentrations, and time since packing.

Perhaps the differences between k_{O2} and k_{DIC} should not be surprising because the stoichiometry of O_2 utilization and DIC accumulation during aerobic respiration can be considerably different than 1:1, depending on the elemental composition and oxidation state of the organic matter metabolized (Rodrigues and Williams 2001, Berggren et al. 2012). The composition of DOC in stream water likely changes seasonally, and the composition of POC in the mesocosms likely changed with time since packing. Thus, changes in the composition of organic C driving hyporheic zone respiration could change the respiratory quotient, and thus obscure relationships of k_{O2} with other factors. This explanation is

consistent with prior studies showing that at summer low flow, the full volume of stream discharge is cycled through the hyporheic zone in as little as 50 m and has a median residence time of 18 h (Kasahara and Wondzell 2003, Wondzell 2011). The mainstem channel is ~700 m long, so stream water would have been cycled through the hyporheic zone many times before being pumped into the mesocosms. When baseflows are higher in the winter and spring, the turnover length of water through the hyporheic zone extends to 200 m or more (Wondzell 2011) and would only cycle through the hyporheic zone a few times before being pumped into the mesocosms. Further, leaf and needle fall in the late autumn and early winter provides fresh organic matter to the stream and supports in-stream production of DOC (Wondzell and Ward 2022), the concentrations of which peak at this time of year (Argerich et al. 2016). Thus, in summer, stream-sourced DOC is likely to be more microbially processed than in winter.

The weak relationship between k_{DIC} and inlet DOC concentrations observed in this study are consistent with other studies showing that metabolic activity may be more strongly related to the bioavailability of the organic compounds present than to the concentration or amount of organic C. Several studies have also shown that, in some streams, much of the DOC in stream water is composed of fractions that are not bioavailable (Brugger et al. 2001, Fischer et al. 2002a, Sobczak and Findlay 2002). We note, however, that both our work and that of Sobczak and Findlay (2002) focused on baseflow periods. Both the concentration of DOC and the proportion of that DOC that is bioavailable may increase with stream discharge, both during storms (Wilson et al. 2013) and seasonally (Fellman et al. 2009), and those conditions should result in a stronger relationship between DOC concentration and hyporheic community respiration. Thus, if our project had sampled over a wider range of conditions, this relationship might have emerged from our data.

Finally, the observed decline in k_{DIC} with time since packing suggests that the bioavailability of buried POC may be declining with time. If the composition of the sediment-bound or buried POC changed over time, these changes might have confounded the relationship between k_{O2} and both the inlet DOC concentrations and time since packing. In this respect, the behavior of the mesocosms mimics the effect of sediment scour and deposition during peak flows. For example, Jones et al. (1995b) showed that elevated levels of hyporheic metabolism followed burial of organic matter in hyporheic sediment during a flood. The buried organic matter accounted for ~15% of hyporheic metabolism immediately after the flood and diminished with time as POC was consumed.

Source of organic C supporting metabolism in the mesocosms

Heterotrophic metabolism in the hyporheic zone is generally assumed to be limited by the amount of bioavailable organic C (Jones 1995). Thus, the supply of DOC transported into the hyporheic zone with stream water is thought to be the primary source of organic C for hyporheic metabolism (Findlay et al. 1993, Jones et al. 1995b, Baker et al. 1999). In general, autochthonous sources of DOC, like algal exudates, are thought to be much more bioavailable than are allochthonous sources from the groundwater or from water draining from adjacent hillslope or riparian soils (Fiebig et al. 1990, Clinton et al. 2010, Wagner et al. 2014). However, DOC leached from leaves and other OM falling directly into the stream may also be readily bioavailable (Dahm 1981, Wiegner et al. 2005, Kaplan et al. 2008). Thus, many studies see high rates of respiration, fueled by DOC, at the proximal end of hyporheic flow paths with much reduced rates at the distal ends of these same flow paths (Brugger et al. 2001, Sobczak and Findlay 2002). Similarly, chamber and column experiments show much higher rates of respiration in downwelling stream water than in upwelling hyporheic water (Findlay et al. 1993).

In some streams, however, respiration can be highly correlated to sediment organic matter content, both in the benthic sediment (Baker 1986, Hedin 1990, Brunke and Fischer 1999, Fischer et al. 2002b) and in the near-stream hyporheic zone (Sobczak et al. 1998, Brugger et al. 2001). Further, high respiration rates are supported in the near-stream sediment by fresh POC entrained from stream water (Fischer et al. 2002b). Despite those observations, the role of sediment-bound or buried POC in supporting heterotrophic metabolism in the hyporheic zone is understudied because POC is assumed to be energetically unfavorable or physically less bioavailable to microbes. Only a handful of studies have compared the role of POC vs DOC in fueling hyporheic metabolism (e.g., Jones et al. 1995b, Brugger et al. 2001, Sobczak and Findlay 2002). A previous study from the well network in WS01 (Corson-Rikert et al. 2016) observed large increases in DIC along hyporheic flow paths without similarly large decreases in DOC, leading the authors to hypothesize that the hyporheic metabolism in WS01 is predominantly driven by POC.

Under our experimental conditions, with flow velocity through the mesocosms set at ~0.2 m/h (to match near-stream flow velocities in the well network), O_2 was never so depleted that respiration became anaerobic. In fact, the lowest O_2 measurement (0.15 mM) was substantially above thresholds for hypoxic (0.063 mM O_2) or anoxic (0.016 mM O_2) conditions (Rounds et al. 2013, Bodamer and Bridgeman 2014). Under these conditions, aerobic respiration of organic C is the most likely explanation for the consistent decreases in the concentrations of dissolved O_2 and increases in the concentration of DIC observed along the flow paths through the mesocosms.

Processes other than aerobic respiration might account for, or contribute to, the production of DIC and consumption of O_2. For example, chemolithotrophs might utilize O_2,

whereas weathering of carbonate minerals might release DIC. However, neither process is likely to be important in our mesocosms. First, the parent materials of the catchment are dominated by siliceous rocks. Thus, DIC is not likely to be generated by weathering of carbonate minerals (Corson-Rikert et al. 2016). Second, chemolithotrophic processes are only likely to dominate hyporheic respiration if the supply of organic C is very low or if the reduction-oxidation conditions of the groundwater are extremely reduced (Storey et al. 1999). These are not the conditions present within the mesocosms. For example, we measured associated analytes in the mesocosms on a single sample date (August 2018), when we measured a mean 0.0074 mM increase in NO_3^- (from 0.022 mM at the inlets to 0.029 mM at the outlets). On this same sample date, mean consumption of O_2 through the 6 mesocosms was 0.1099 mM so that nitrification, which consumes at most 2 mol O_2/mol N (Rodrigues and Williams 2001), would account for no more than 14% of the observed change in O_2. Oxidation of reduced P and S compounds could also consume O_2, but they only showed small changes in concentration over the 2-m long flow paths, with PO_4 increasing by 0.00070 mM and SO_4 decreasing by 0.00062 mM, on average. These results are consistent with previous studies conducted at the WS01 well network showing that stream and subsurface riparian waters are low in concentrations of the reduced substances commonly used by chemolithotrophs. Therefore, the O_2 loss from chemolithotrophy is unlikely to substantially influence overall O_2 decline along flow paths through our mesocosms.

The observed O_2 loss and concomitant increase in DIC suggest aerobic metabolism. However, determining the relative importance of stream-sourced DOC or sediment-bound or buried POC for metabolism is difficult. Microbial processes can continually generate DOC from POC, respire DOC, or fix DOC back into POC (Wiegner et al. 2005). Further, a complex range of organic matter compounds are present, so stoichiometric relationships are likely to differ from 1:1, depending on the elemental composition and oxidation state of the organic matter metabolized.

We can only evaluate the likely sources of organic C based on gross inputs and net changes in the concentration of DOC. Based on gross inputs of DOC in stream water and assuming a 1:1 stoichiometry, the stream water does not supply sufficient DOC to the mesocosms to account for the losses of O_2 and gains in DIC observed in the summer–autumn samples. Thus, at this time of year when temperatures are high and DOC concentrations are low in stream water, organic C ultimately derived from POC must be an important resource for community metabolism. Although gross inputs of stream-sourced DOC would be sufficient to account for the losses of O_2 and gains in DIC observed in the winter–spring, other factors suggest that stream-sourced DOC is not the primary source of organic C for hyporheic metabolism. First, net changes in DOC through the 2-m mesocosms are very small at all times of year. It seems unlikely that microbial production of DOC from POC would consistently match the consumption of DOC, so that net changes are always small. Second, if hyporheic zone metabolism was controlled by supply of bioavailable stream-sourced DOC, we would expect to see steep drops in O_2 and steep production of DIC at the proximal ends of flow paths, as well as gradual flattening of these curves further along the flow path as the system became increasingly limited by DOC delivered from the stream. Instead, we observed linear changes in DOC, DIC, and O_2 concentrations with travel time over the length of the mesocosms, and these changes were best fit with zero-order kinetic reactions. More recently, the mesocosm has been reconfigured to simulate a single 12-m-long hyporheic flow path, and it also shows linear changes in concentrations with time that were best fit with zero-order kinetic reactions (S. Herzog, Oregon State University, Cascades Campus, Bend, Oregon, USA, personal communication). Finally, k_{DIC} decreased with time since packing of the mesocosms, which would not be expected if stream-sourced DOC was the primary source of organic C for hyporheic metabolism. Overall, these results suggest that hyporheic community respiration in the mesocosms has limited dependence on import of DOC from surface waters. Rather, the processes that release bioavailable DOC from sediment-bound or buried POC may well govern the rates of hyporheic zone metabolism, and these processes appear relatively constant with distance along hyporheic zone flow paths.

If POC is the primary source of organic C for hyporheic metabolism as our data suggest, organic matter would either have been packed into the mesocosms when they were initially filled with native streambed sediment in May 2016 or resulted from growth and subsequent turnover of biofilms on sediment surfaces within the mesocosms. The accumulation of biomass within the mesocosms is an unlikely source of organic C to fuel heterotrophic metabolism during our sample periods. First, we made every effort to keep the mesocosms at an equilibrium state. We constantly pumped stream water through each mesocosm at a rate of 48 mL/min (~20 cm/h) since the mesocosms were first packed. Of course, streamwater DOC concentration and composition varied over that time, so it is possible that microbial biomass could accumulate during periods with high DOC availability that would be followed by death and respiration of the accumulated biomass during periods when DOC supplied in stream water was insufficient to meet metabolic demands. However, our samples span a 2-y period, multiple seasons, and a variety of instream conditions. Additionally, on all sample dates, the consumption of O_2 and the production of DIC were much greater than expected from the net change in DOC, suggesting that the excess metabolism was consistent over time and did not vary seasonally as would be expected if biomass was accumulating and subsequently

being turned over. Thus, stored, sediment-bound or buried POC appears to be the predominant source of organic C driving heterotrophic metabolism in the mesocosms.

Streams range widely in the relative contributions of stream-sourced DOC vs sediment-bound or buried POC supporting hyporheic metabolism (Findlay et al. 1993, Sobczak and Findlay 2002, Zarnetske et al. 2011), with published values ranging from as little as 35% (Brugger et al. 2001) to as much as 85% (Jones et al. 1995b). Hedin (1990) showed that benthic community respiration was highly correlated to sediment organic matter content, weakly correlated to temperature, and uncorrelated to DOC. Agreement between his results and other studies in forested streams led him to hypothesize that POC would be the primary source of organic C for heterotrophic respiration in shaded forested streams where allochthonous inputs are large relative to autochthonous production. Our results for WS01 appear to agree with those of Hedin (1990) and results he cites from other forested stream systems. Even so, our results are quite extreme, with POC potentially supplying >90% of the organic matter needed to account for the amount of hyporheic respiration during summer low-flow periods, estimated from change in O_2.

Previous work at WS01 has documented very high rates of hyporheic exchange flows, with estimated turnover lengths of stream water through the hyporheic zone ranging from 50 to 130 m under late summer baseflow conditions. Even under high baseflows during the wet season, turnover lengths are only 250 m (Kasahara and Wondzell 2003, Wondzell 2011) Such repetition of surface–subsurface exchange flows would result in accumulation of highly processed C as bioavailable fractions are stripped along hyporheic flow paths (Sobczak and Findlay 2002). Thus, bioavailable DOC would have little opportunity to accumulate in the stream water, whether from autochthonous production or leaching of allochthonous particulate OM. This lack of bioavailable stream-sourced DOC would explain the rates of hyporheic zone metabolism we observed at WS01, both in the mesocosms and the well field, which were ~100× slower than those reported by Jones et al. (1995b) and Pusch (1996). The lack of bioavailable stream-sourced DOC would also explain the linear patterns of O_2 consumption and DIC production we observed along our 2-m flow paths through the mesocosms.

The relative importance of stream-sourced DOC versus sediment-bound or buried POC varied seasonally in the mesocosms, with net changes in stream-sourced DOC accounting for only 7 to 29% of the hyporheic metabolism in the summer–autumn and 24 to 77% in the winter–spring, relative to the consumption of O_2 and production of DIC. These differences likely resulted from a combination of seasonal changes in the amount and composition of DOC and the underlying metabolic rate. Streamwater DOC concentrations tend to be higher in winter–spring than in summer–autumn, although they peak in late autumn during and immediately after the period of leaf fall. Further, respiration rates tend to be temperature dependent (Jankowski et al. 2014, Vieweg et al. 2016), so we would expect hyporheic metabolic rates to be lower over the winter–spring period when water temperatures are colder. Thus, with lower metabolic rates and higher concentration of DOC that is, perhaps, more bioavailable, we would expect DOC to satisfy organic C demand more completely in the winter. Together, these factors likely explain the seasonal differences, with sediment-bound or buried POC being the dominant source of organic matter for hyporheic respiration in summer-autumn but with increasing importance of DOC in winter-spring.

ACKNOWLEDGEMENTS

Author contributions: RH, SMW, KF, and DT developed the overall direction of the research and wrote the proposal that funded the work; SMW led the development of the mesocosm facility with substantial design contributions by RH, RP, and WRJ; SPS operated and maintained the mesocosm facility with help from SMW, RH, RP, AS, and WJR; SPS wrote the 1st draft of this manuscript with careful editing and revisions by SMW with subsequent editing and comments by RH, RP, KF, DT, and WJR.

We thank Oregon State University's College of Earth, Ocean, and Atmospheric Sciences machinist, Ben Russell for helping design and then build the mesocosms. We also thank the Journal's Associate Editor, Dr. R. Payn, and 2 anonymous reviewers for edits and comments that helped improve the paper. This research was funded by the National Science Foundation (EAR-1417603) and the United States Forest Service, Pacific Northwest Research Station. Data from this study are archived in the H. J. Andrews Databank (CF011: http://andlter.forestry.oregonstate.edu/data/abstract.aspx?dbcode=CF011 and CF016: http://andlter.forestry.oregonstate.edu/data/abstract.aspx?dbcode=CF016). Additional data were provided by the H. J. Andrews Experimental Forest and Long-Term Ecological Research program, administered cooperatively by the United States Department of Agriculture Forest Service, Pacific Northwest Research Station, Oregon State University, and the Willamette National Forest. This material is based upon work supported by the National Science Foundation under Grant No. DEB-1440409. H. J. Andrews datasets used for exploratory use are:

HF004, doi.:10.6073/pasta/c85f62e9070a4ebe5e455190b4879c0c,

MS001, doi.org:10.6073/pasta/c021a2ebf1f91adf0ba3b5e53189c84f.

Note that the use of trade or firm names in this publication is for reader information and does not imply endorsement by the United States Department of Agriculture of any product or service.

LITERATURE CITED

Argerich, A., R. Haggerty, S. L. Johnson, S. M. Wondzell, N. Dosch, H. Corson-Rikert, L. R. Ashkenas, and R. Pennington. 2016. Comprehensive multiyear carbon budget of a temperate headwater stream. Journal of Geophysical Research G: Biogeosciences 121:1306–1315.

Baker, J. H. 1986. Relationship between microbial activity of stream sediments, determined by three different methods, and abiotic variables. Microbial Ecology 12:193–203.

Baker, M. A., C. N. Dahm, and H. M. Valett. 1999. Acetate retention and metabolism in the hyporheic zone of a mountain stream. Limnology and Oceanography 44:1530–1539.

Baker, M. A., H. M. Valett, and C. N. Dahm. 2000. Organic carbon supply and metabolism in a shallow groundwater ecosystem. Ecology 81:3133–3148.

Battin, T. J. 1999. Hydrologic flow paths control dissolved organic carbon fluxes and metabolism in an alpine stream hyporheic zone. Water Resources Research 35:3159–3169.

Battin, T. J., L. A. Kaplan, J. D. Newbold, and S. P. Hendricks. 2003. A mixing model analysis of stream solute dynamics and the contribution of a hyporheic zone to ecosystem function. Freshwater Biology 48:995–1014.

Berggren, M., J. F. Lapierre, and P. A. Del Giorgio. 2012. Magnitude and regulation of bacterioplankton respiratory quotient across freshwater environmental gradients. ISME Journal 6:984–993.

Bodamer, B. L., and T. B. Bridgeman. 2014. Experimental dead zones: Two designs for creating oxygen gradients in aquatic ecological studies. Limnology and Oceanography: Methods 12:441–454.

Brugger, A., B. W., I. Kolar, B. Reitner, and G. J. Herndl. 2001. Immobilization and bacterial utilization of dissolved organic carbon entering the riparian zone of the alpine Enns River, Austria. Aquatic Microbial Ecology 24:129–142.

Brunke, M., and H. Fischer. 1999. Hyporheic bacteria – Relationships to environmental gradients and invertebrates in a prealpine stream. Archiv fur Hydrobiologie 146:189–217.

Cardenas, M. B., and J. L. Wilson. 2006. The influence of ambient groundwater discharge on exchange zones induced by current–bedform interactions. Journal of Hydrology 331:103–109.

CCAL (Cooperative Chemical Analytical Laboratory). 2013. CCAL Standard Operating Procedures, Oregon State University and United States Forest Service Cooperative Chemical Analytical Laboratory, Corvallis, Oregon. (Available from: http://ccal.oregonstate.edu/sops, accessed July 2014)

Clinton, S. M., R. T. Edwards, and S. E. Findlay. 2010. Exoenzyme activities as indicators of dissolved organic matter composition in the hyporheic zone of a floodplain river. Freshwater Biology 55:1603–1615.

Corson-Rikert, H. A., S. M. Wondzell, R. Haggerty, and M. V. Santelmann. 2016. Carbon dynamics in the hyporheic zone of a headwater mountain stream in the Cascade Mountains, Oregon. Water Resources Research 52:7556–7576.

Dahm, C. N. 1981. Pathways and mechanisms for removal of dissolved organic carbon from leaf leachate in streams. Canadian Journal of Fisheries and Aquatic Science 38:68–76.

Daly, C., M. Schulze, and W. McKee. 2019. Meteorological data from benchmark stations at the HJ Andrews Experimental Forest, 1957 to present. Forest Science Data Bank, Corvallis, Oregon. (Available from: http://andlter.forestry.oregonstate.edu/data/abstract.aspx?dbcode = MS001)

Fellman, J. B., E. Hood, D. V. D'Amore, R. T. Edwards, and D. White. 2009. Seasonal changes in the chemical quality and biodegradability of dissolved organic matter exported from soils to streams in coastal temperate rainforest watersheds. Biogeochemistry 95:277–293.

Fiebig, D. M., M. A. Lock, and C. Neal. 1990. Soil water in the riparian zone as a source of carbon for a headwater stream. Journal of Hydrology 116:217–237.

Findlay, S., and W. V. Sobczak. 1996. Variability in removal of dissolved organic carbon in hyporheic sediments. Journal of the North American Benthological Society 15:35–41.

Findlay, S., D. Strayer, C. Goumbala, and K. Gould. 1993. Metabolism of stream water dissolved organic carbon in the shallow hyporheic zone. Limnology and Oceanography 38:1493–1499.

Fischer, H., A. Sachse, C. E. W. Steinberg, and M. Pusch. 2002a. Differential retention and utilization of dissolved organic carbon by bacteria in river sediments. Limnology and Oceanography 47:1702–1711.

Fischer, H., S. C. Wanner, and M. Pusch. 2002b. Bacterial abundance and production in river sediments as related to the biochemical composition of particulate organic matter (POM). Biogeochemistry 61:37–55.

Folk, R. L. 1974. Petrology of sedimentary rocks. Hemphill Publishing Company, Austin, Texas.

Grimm, N. B., and S. G. Fisher. 1984. Exchange between interstitial and surface water: Implications for stream metabolism and nutrient cycling. Hydrobiologia 111:219–228.

Harvey, J. W., and K. E. Bencala. 1993. The effect of streambed topography on surface- subsurface water exchange in mountain catchments. Water Resources Research 29:89–98.

Hedin, L. O. 1990. Factors controlling sediment community respiration in woodland stream ecosystems. Oikos 57:94–105.

Hedin, L. O., J. C. von Fischer, N. E. Ostrom, B. P. Kennedy, M. G. Brown, and G. P. Robertson. 1998. Thermodynamic constraints on nitrogen transformations and other biogeochemical processes at soil–stream interfaces. Ecology 79:684–703.

Helton, A. M., M. S. Wright, E. S. Bernhardt, G. C. Poole, R. M. Cory, and J. A. Stanford. 2015. Dissolved organic carbon lability increases with water residence time in the alluvial aquifer of a river floodplain ecosystem. Journal of Geophysical Research: Biogeosciences 120:693–706.

Hester, E. T., B. M. Cardenas, R. Haggerty, and S. V. Apte. 2017. The importance and challenge of hyporheic mixing. Water Resources Research 53:3565–3575.

Hitchcock, C. L., and A. Cronquist. 1973. Flora of the Pacific Northwest. University of Washington Press, Seattle, Washington.

Hoogsteen, M. J. J., E. A. Lantinga, E. J. Bakker, J. C. J. Groot, and P. A. Tittonell. 2015. Estimating soil organic carbon through loss on ignition: Effects of ignition conditions and structural water loss. European Journal of Soil Science 66:320–328.

Jankowski, K., D. E. Schindler, and P. J. Lisi. 2014. Temperature sensitivity of community respiration rates in streams is associated with watershed geomorphic features. Ecology 95:2707–2714.

Johnson, S., S. Wondzell, and J. Rothacher. 2020. Stream discharge in gaged watersheds at the HJ Andrews Experimental Forest, 1949 to present. Forest Science Data Bank, Corvallis, OR. Available: http://andlter.forestry.oregonstate.edu/data/abstract.aspx?dbcode = HF004.

Jones Jr, J. B. 1995. Factors controlling hyporheic respiration in a desert stream. Freshwater Biology 34:91–99.

Jones Jr, J. B., S. G. Fisher, and N. B. Grimm. 1995a. Nitrification in the hyporheic zone of a desert stream ecosystem. Journal of the North American Benthological Society 14:249–258.

Jones Jr, J. B., S. G. Fisher, and N. B. Grimm. 1995b. Vertical hydrologic exchange and ecosystem metabolism in a Sonoran Desert stream. Ecology 76:942–952.

Kaplan, L. A., T. N. Wiegner, J. D. Newbold, P. H. Ostrom, and H. Gandhi. 2008. Untangling the complex issue of dissolved organic carbon uptake: A stable isotope approach. Freshwater Biology 53:855–864.

Kasahara, T., and S. M. Wondzell. 2003. Geomorphic controls on hyporheic exchange flow in mountain streams. Water Resources Research 39:1005.

Malzone, J. M., S. K. Anseeuw, C. S. Lowry, and R. Allen-King. 2016. Temporal hyporheic zone response to water table fluctuations. Groundwater 54:274–285.

Mermillod-Blondin, F., L. Mauclaire, and B. Montuelle. 2005. Use of slow filtration columns to assess oxygen respiration, consumption of dissolved organic carbon, nitrogen transformations, and microbial parameters in hyporheic sediments. Water Research 39:1687–1698.

Nakamura, F., and F. J. Swanson. 1993. Effects of coarse woody debris on morphology and sediment storage of a mountain stream system in western Oregon. Earth Surface Processes and Landforms 18:43–61.

Naiman, R. J., and J. R. Sedell. 1979. Characterization of particulate organic matter transported by some Cascade mountain streams. Journal of the Fisheries Research Board of Canada 36:17–31.

Pennington, R. S. 2019. Measurement of gas exchange, stream metabolism, and carbon fluxes of headwater streams. MS Thesis. Oregon State University, Corvallis, Oregon. (Available from: https://ir.library.oregonstate.edu/concern/graduate_thesis_or_dissertations/kh04dw66q)

Poole, G. C., J. A. Stanford, S. W. Running, and C. A. Frissell. 2006. Multiscale geomorphic drivers of groundwater flow paths: Subsurface hydrologic dynamics and hyporheic habitat diversity. Journal of the North American Benthological Society 25:288–303.

Pusch, M. 1996. The metabolism of organic matter in the hyporheic zone of a mountain stream, and its spatial distribution. Hydrobiologia 323:107–118.

Rodrigues, R. M. N. V., and P. J. le B. Williams. 2001. Heterotrophic bacterial utilization of nitrogenous and nonnitrogenous substrates, determined from ammonia and oxygen fluxes. Limnology and Oceanography 46:1675–1683.

Rounds, S. A., F. D. Wilde, and G. F. Ritz. 2013. Dissolved oxygen (ver. 3.0). Techniques of Water-Resources Investigations. Book 9, Chapter A6.2. United States Geological Survey, Reston, Virginia. (Available from: https://doi.org/10.3133/twri09A6.2)

Schindler, J. E., and D. P. Krabbenhoft. 1998. The hyporheic zone as a source of dissolved organic carbon and carbon gases to a temperate forested stream. Biogeochemistry 43:157–174.

Schmadel, N. M., A. S. Ward, and S. M. Wondzell. 2017. Hydrologic controls on hyporheic exchange in a headwater mountain stream. Water Resources Research 53:6260–6278.

Serchan, S. P. 2021. Controls on inorganic and organic carbon biogeochemistry in the hyporheic zone of a headwater mountain stream using two approaches: Well-network and hyporheic mesocosms. MS Thesis. Oregon State University, Corvallis, Oregon. (Available from: https://ir.library.oregonstate.edu/concern/graduate_thesis_or_dissertations/9019s9306)

Shibata, H., H. Mitsuhashi, Y. Miyake, and S. Nakano. 2001. Dissolved and particulate carbon dynamics in a cool-temperate forested basin in northern Japan. Hydrological Processes 15: 1817–1828.

Sobczak, W. V., and S. Findlay. 2002. Variation in bioavailability of dissolved organic carbon among stream hyporheic flow paths. Ecology 83:3194–3209.

Sobczak, W. V., L. O. Hedin, and M. J. Klug. 1998. Relationships between bacterial productivity and organic carbon at a soil–stream interface. Hydrobiologia 386:45–53.

Stegen, J. C., J. K. Fredrickson, M. J. Wilkins, A. E. Konopka, W. C. Nelson, E. V. Arntzen, W. B. Chrisler, R. K. Chu, R E. Danczak, S. J. Fansler, D. W. Kennedy, C. T. Resch, and M. Tfaily. 2016. Groundwater–surface water mixing shifts ecological assembly processes and stimulates organic carbon turnover. Nature Communications 7:11237.

Storey, R. G., R. R. Fulthorpe, and D. D. Williams. 1999. Perspectives and predictions on the microbial ecology of the hyporheic zone. Freshwater Biology 41:119–130.

Tsypin, M., and G. L. Macpherson. 2012. The effect of precipitation events on inorganic carbon in soil and shallow groundwater, Konza Prairie LTER Site, NE Kansas, USA. Applied Geochemistry 27:2356–2369.

Vieweg, M., M. J. Kurz, N. Trauth, J. H. Fleckenstein, A. Musolff, and C. Schmidt. 2016. Estimating time-variable aerobic respiration in the streambed by combining electrical conductivity and dissolved oxygen time series. Journal of Geophysical Research: Biogeosciences 121:2199–2215.

Voltz, T., M. Gooseff, A. S. Ward, K. Singha, M. Fitzgerald, and T. Wagener. 2013. Riparian hydraulic gradient and stream-groundwater exchange dynamics in steep headwater valleys. Journal of Geophysical Research: Earth Surface 118:953–969.

Wagner, K., M. M. Bengtsson, K. Besemer, A. Sieczko, N. R. Burns, E. R. Herberg, and T. J. Battin. 2014. Functional and structural responses of hyporheic biofilms to varying sources of dissolved organic matter. Applied and Environmental Microbiology 80:6004–6012.

Ward, A. S., M. Fitzgerald, M. N. Gooseff, T. J. Voltz, A. M. Binley, and K. Singha. 2012. Hydrologic and geomorphic controls on hyporheic exchange during base flow recession in a headwater mountain stream. Water Resources Research 48:W04513.

Ward, A. S., N. M. Schmadel, S. M. Wondzell, C. Harman, M. N. Gooseff, and K. Singha. 2016. Hydrogeomorphic controls on hyporheic and riparian transport in two headwater mountain streams during base flow recession. Water Resources Research 52:1479–1497.

Wiegner, T. N., L. A. Kaplan, J. D. Newbold, and P. H. Ostrom. 2005. Contribution of dissolved organic C to stream metabolism: A mesocosm study using ^{13}C-enriched tree tissue leachate. Journal of the North American Benthological Society 24:48–67.

Wilson, H. F., J. E. Saiers, P. A. Raymond, and W. V. Sobczak. 2013. Hydrologic drivers and seasonality of dissolved organic carbon concentration, nitrogen content, bioavailability, and export in a forested New England stream. Ecosystems 16: 604–616.

Wondzell, S. M. 2006. Effect of morphology and discharge on hyporheic exchange flows in two small streams in the Cascade Mountains of Oregon, USA. Hydrological Processes 20:267–287.

Wondzell, S. M. 2011. The role of the hyporheic zone across stream networks. Hydrological Processes 25:3525–3532.

Wondzell, S. M., and M. N. Gooseff. 2013. Geomorphic controls on hyporheic exchange across scales – Watersheds to particles. Pages 203–218 *in* J. Shroder and E. Wohl (editors). Treatise on geomorphology. Volume 9. Academic Press, San Diego, California.

Wondzell, S. M., and F. J. Swanson. 1999. Floods, channel change, and the hyporheic zone. Water Resources Research 35:555–567.

Wondzell, S. M., and A. S. Ward. 2022. The channel-source hypothesis: Empirical evidence for in-channel sourcing of dissolved organic carbon to explain hysteresis in a headwater mountain stream. Hydrological Processes 36:e14570.

Zarnetske, J. P., R. Haggerty, S. M. Wondzell, and M. A. Baker. 2011. Dynamics of nitrate production and removal as a function of residence time in the hyporheic zone. Journal of Geophysical Research 116:G01025.